Automatic Field Distribution Measurement inside of Enclosures

Hans A. Wolfsperger, Dietmar Jordan, Adolf J. Schwab
Institute for Electric Energy Systems and High Voltage Technologie
University of Karlsruhe, Kaiserstraße 12, 76128 Karlsruhe, Germany.
email: wolfsperger@ieh.etec.uni-karlsruhe.de

Abstract: A new measurement system is developed to determine the field distribution inside of enclosures, shielded cabinets etc. It consists of a small electric or magnetic field sensor and a mechanism which allows to position this sensor with an accuracy of 1 mm in three axes. Full automatic field intensity and shielding effectiveness measurements can be performed at any position in the frequency range 30 MHz – 1 GHz, obtaining three-dimensional images of the field. Thus, weak points of the shield and field extrema caused by cavity resonances can be detected.

Introduction

Up to now, the quantity *Shielding Effectiveness* SE is used to describe the shielding properties of enclosures. SE usually is determined by insertion loss measurement, described e .g. in MIL-STD 285 or IEEE 299. Two measurements with a illuminated E- or H-field sensor are performed: With and without shielding structure around the sensor, fig. 1.

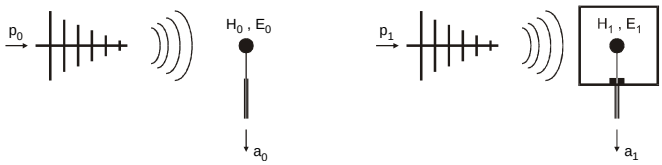

Fig. 1: Insertion loss measurement, conventional method to determine shielding effectiveness.

The shielding effectiveness is defined as the difference of levels

$$SE = a_0 - a_1, \qquad (1)$$

while the input power level is kept constant.

Normally the sensor is placed in the centre of the enclosure. This method has several disadvantages:

- Depending on the test site, the field strength at the shielding surface may vary although the same reference level is measured with the receiving antenna (non-uniformity of the field).
- The information of the field inside of the examined enclosure is reduced to only one value.
- Apertures in the shield and cavity resonances cause a very irregular field, so the results are varying, depending on the arbitrary position of the receiving antenna inside.

The last point is maybe most important. Using reflected dipoles, the field distribution inside of an enclosure can be calculated. Fig. 2 shows a 3d-plot of the calculated electric field strength in a cross-section of a shielded cabinet. The excitation occures in the resonance frequency through a hole at the front.

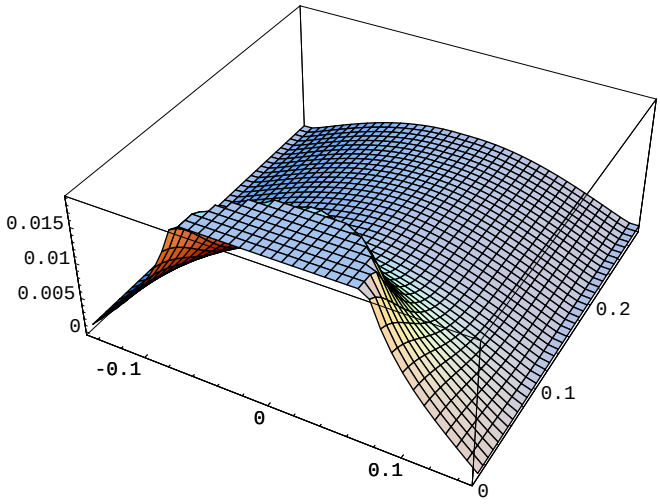

Fig. 2: Magnitude of the electric field strength inside of an enclosure, excited by an aperture at the front. 110 resonance.

To overcome these insufficiencies and to get a image of the field distribution (in order to place critical components at the best point), a field measurement system has been developed, which allows to determine the electric or magnetic field strength at any point inside of an enclosure. It consists of a field sensor (a small electric or magnetic antenna), a sensor positioning device, a control unit and a power supply, fig. 3. Signal source and test receiver are controlled by a PC, which is in dialog with the control unit. The PC also carries out data processing after the measurement, which can be performed in an anechoic or mode-stirred chamber.

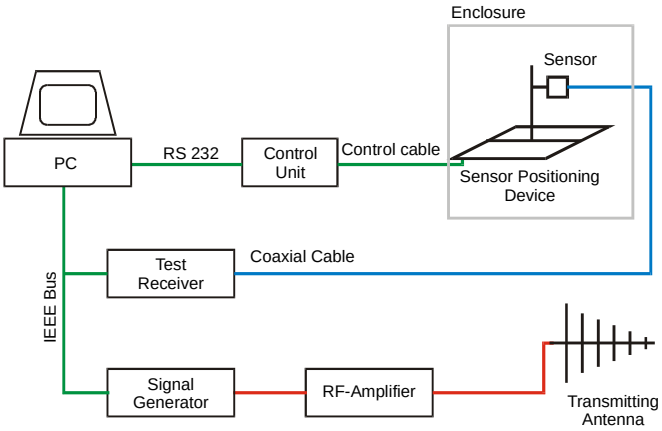

Fig. 3: Complete measurement system.

The sensor positioning device places the sensor at a definite position inside of the enclosure. It is controlled by the control unit outside of the test site (anechoic chamber, MSC).

E- and H-Field Sensors

Different types of electricially short sensors can be used, some are shown in fig. 4.

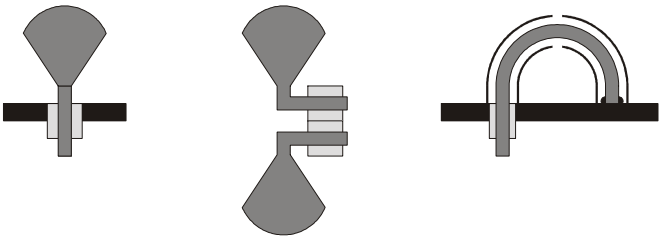

Fig. 4: a) monopole, b) dipole and c) loop sensor.

The sensors are used beyond their first resonance, providing a linear frequency characteristic, Fig. 5.

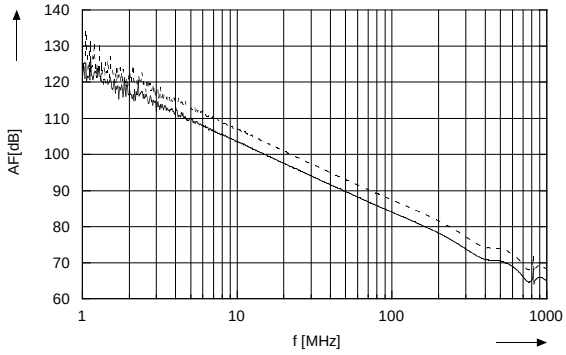

Fig. 5: Antenna factor (E/U) of monopoles, shown in figure 4 a).

For the dipole (fig. 4 b), a balun is necessary to connect it to the coaxial input port of the test receiver. This is a problem, because the dipole has a large bandwich, while it is difficult to find baluns with the necessary frequency range.

The antenna factor was determined in a Coaxial TEM-Cell, with first resonance at 806 MHz. The non-linearities of the frequency characteristic, starting at 400 MHz are caused by insufficiencies of this cell.

Sensor Positioning Device

The sensor positioning device, fig. 6, made of synthetic material, allows to move the small field sensor with a position accuracy of 1 mm. The dimensions of the whole mechanism are variable, so it can be build in into enclosures of different size. First measurement were performed in a shielded cabinet, 60 x 60 x 120 cm³, but smaller or lager dimensions are possible.

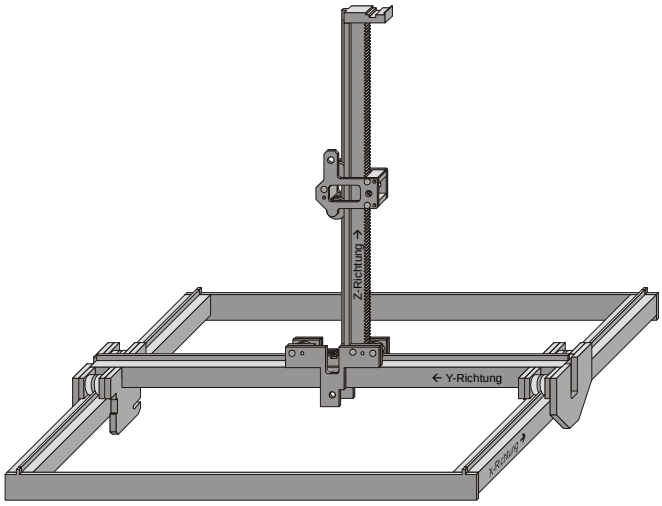

Fig. 6: Sensor positioning device.

Metal parts has been avoided; only the drives – small, geared motors – and some wires are metallic. The rack and pinion drives for all three axes are made from acetate. Fig. 7 is a photo of the sensor positioning device with connected control unit. During the measurement the control unit (connected box) is outside of the test chamber, therefore a control cable has to be layed and passed through into the enclosure under test.

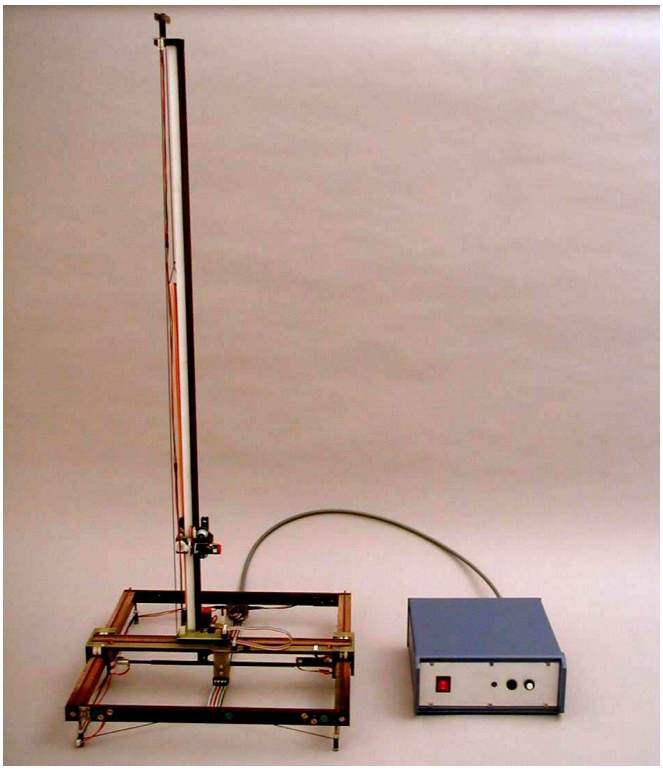

Fig. 7: Sensor positioning device and control unit.

To determine the sensor's position, light barriers integrated in the carriages sample the perforated tracks. Other light barriers serve as limit switches. The sensor can be mounted on the carriage for the vertical direction, shown in fig. 8. One can see the angular drive, the DC-motor, the guide wheels and the index holes in the rack.

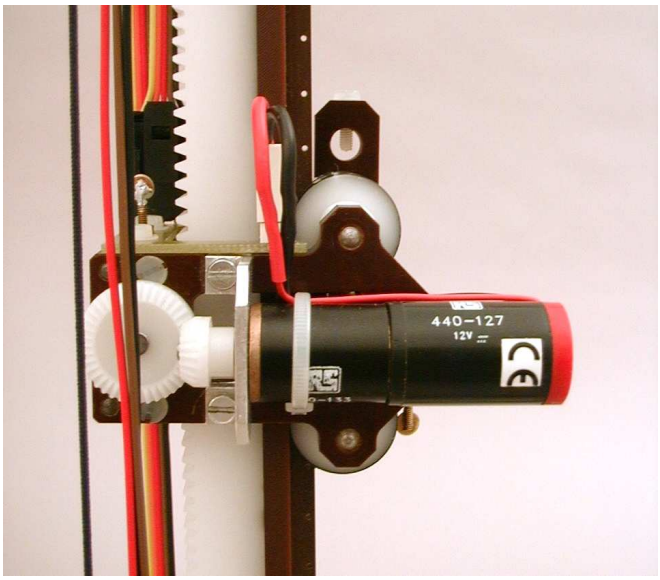

Fig. 8: Carriage for vertical direction.

Unfortunately, wires could not be avoided. To suppress interference of the measurement by resonances on the wires, ferrites has been attached to all cables. Nevertheless, the unavoidable metal parts distort the electric field. To reduce the repercussion, a photonic sensor could be used, avoiding metal parts and wires and using an optical waveguide instead of a coaxial cable. Its disadvantages are very high costs and a lower sensitivity.

Control Unit

The drives are swiched by a micro-controller in the control unit, Fig. 9.

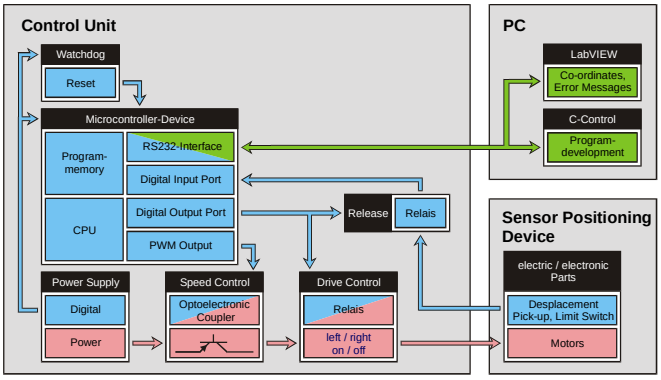

Fig. 9: Block diagram of the control unit.

It also evaluates the signals from the light barriers which are used to determine the position of the moving parts. The control unit communicates with the PC via RS 232 connection, e. g. it receives position data and sends the actual position after the sensor has moved. Because there are no time-critical processes, the micro-controller is programmed in BASIC, allowing fast software development and easy maintenance. Fig. 10 shows the simplified algorithm for moving the sensor.

To increase the precision of sensor movement and to reduce oscillations, the software allows to accelerate the carriages in a smooth way. Therefore, the drive speed is in- or decremented stepwise. The maximum velocity depends on the distance between start position and target position.

The algorithms for speed adjustment, initialisation, and galvanic separation during the measurement are not shown in the flow chart fig. 10 for clear lay-out reasons.

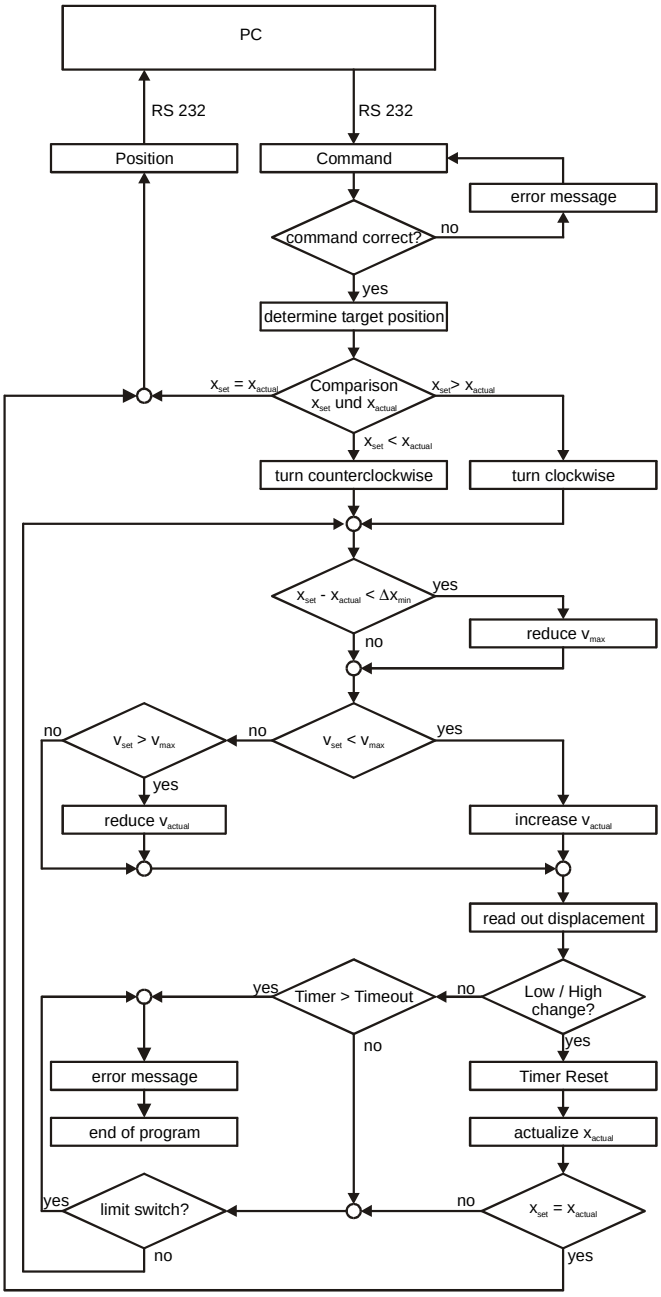

Fig 10: Flow chart of the control unit's program.

Measurement Procedure

The whole measurement procedure is controlled by the PC, which controls all measurement devices via IEEE-Bus and processes the measured data. To get a three-dimensional image of the shielding effectiveness of an enclosure, the steps are as shown in the flow chart, fig 11:

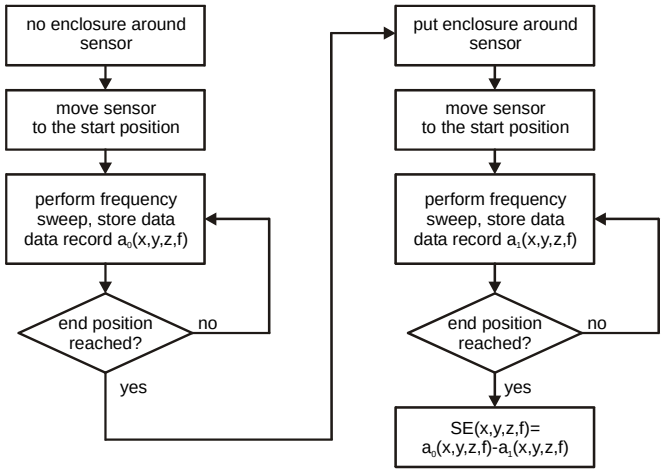

Fig. 11: Flow chart of the measurement procedure to get a three-dimensional image of the SE.

Conclusion

A new measurement system allows to determine the field distribution inside of enclosures.

Full automatic field intensity and shielding effectiveness measurements can be performed to obtain three-dimensional images.

To reduce the repercussion of the measurement set-up, it is planned to replace even more matallic parts, especially the cables.

Futur work is to perform a variety of different measurements, comparing the results to calculated ones.

References

[1] White, D. R. J. and Mardiguan, M., „Electromagnetic Shielding“, Handbook Series on Electromagnetic Interference an Compatibility, Vol. 3., 1988.

[2] IEEE Std 299, 1997.

[3] MIL-Std-285, US Dept. of Defence, 1956.

[4] VG Norm 95373, Part 15 (German standard for defence devices), 1978.

[5] Braun, Ch., Guidi, P., Schmidt, H.U., Elektrisch kurze Antennen zur Feldmessung, FhG-Bericht, 1996.